Visualization of the Process of Static Buckling of a Micropolar Meshed Cylindrical Panel[*]

Ekaterina Krylova[1] [0000-0002-7593-0320], Irina Papkova[2] [0000-0003-4062-1437] and

Vadim Krysko[2] [0000-0002-4914-764X]

[1] Saratov State University, 83 Astrakhanskaya Street, Saratov, 410012
[2] Yuri Gagarin State Technical University of Saratov, 77 Politechnicheskaya street, Saratov, Russia, 410054
Kat.krylova@bk.ru, ikravzova@mail.ru, tak@san.ru

Abstract. Process visualization of static stability loss in mechanics is shown by the micropolar meshed cylindrical panel example with two families of mutually perpendicular ribs. The mathematical model of the panel's behavior is based on the Kirchhoff-Love hypotheses. The micropolar theory is applied to account for scale effects. Geometric nonlinearity is taken into account according to the theory of Theodor von Karman. The mesh structure is taken into account based on the Pshenichnov I. G. continuum model. Visualization of numerical results using Autodesk 3ds Max software made it possible to more clearly assess the phenomenon of static buckling of the shell in question. Visualization of the results using 3D made it possible to establish that an increase in the distance between the edges of the mesh panel and an increase in the parameter depending on the size does not change the bending shape of the panel, as well as the diagrams of moments and forces at subcritical and supercritical loads.

Keywords: Meshed Panel, Micropolar Theory, Buckling, Geometric Nonlinearity.

1   Introduction

Subsequent paragraphs, however, are indented Meshed structural elements are widely used in engineering practice. The development of nano-technologies leads to supplement of studying the behavior of meshed elements at the micro- and nano-scale level. [1-4]. The nowaday question is qualitative visualization of the results of numerical experiments [5-6]. The presentation of the results of numerical experiments not in tabular form, but in the form of 2D and 3D graphs will allow the deeper understanding

of the behavior of elements of mechanical structures under the influence of various kinds of factors. The description of the meshed structure of the structural elements is mainly based on two design models: continuous [7-8] and discrete [9-12]. Such theories as the micropolar moment theory of elasticity [13-16], the nonlocal theory of elasticity [17-19], the gradient theory of elasticity [20] and surface elasticity [21] are being developed today for to simulate scale effects in the continuum.

Today, there is a large number of studies of the full-sized statics and dynamics of the meshed structures [7, 8, 11, 22]. However, there are very few works devoted to the study of the behavior of the meshed plates and shells based on theories which are built on the effects of scale. [23-26].

2 Problem statement

The object of study is a shallow cylindrical panel rectangular in plan, which occupies an area $\Omega = \left\{-c \leq x \leq c; -b \leq y \leq b; -\dfrac{h}{2} \leq z \leq \dfrac{h}{2}\right\}$ in space R^3. The nonzero components of the strain tensor in the case of Kirchhoff – Love hypotheses and T. von Karman's theory can be written as:

$$e_{xx} = \frac{\partial u}{\partial x} + \frac{1}{2}\left(\frac{\partial w}{\partial x}\right)^2 - z\frac{\partial^2 w}{\partial x^2}; \; e_{xy} = \frac{1}{2}\left(\frac{\partial u}{\partial y} + \frac{\partial v}{\partial x} + \frac{\partial w}{\partial x}\frac{\partial w}{\partial y}\right) - z\frac{\partial^2 w}{\partial x \partial y},$$

$$e_{yy} = \frac{\partial v}{\partial y} + \frac{1}{2}\left(\frac{\partial w}{\partial y}\right)^2 - k_y w - z\frac{\partial^2 w}{\partial y^2}; \tag{1}$$

here u, v, w are axial displacements of the middle surface of the plate in the directions x, y, z respectively, k_y is geometric parameter of curvature. The panel material is considered as Cosserat pseudo-continuum with cramped rotation of the particles. Along with the stress field, the moment stresses are also taken into account. It is assumed that the fields of displacements and rotations are not independent. The components of the symmetric bending-torsion tensor, taking into account of the accepted hypotheses and assumptions, can be written as follows:

$$\chi_{xx} = \frac{\partial^2 w}{\partial x \partial y}; \; \chi_{yy} = -\frac{\partial^2 w}{\partial y \partial x}; \; \chi_{xy} = \frac{1}{2}\left(\frac{\partial^2 w}{\partial y^2} - \frac{\partial^2 w}{\partial x^2}\right); \; \chi_{xz} = \frac{1}{4}\left(\frac{\partial^2 v}{\partial x^2} - \frac{\partial^2 u}{\partial x \partial y}\right);$$

$$\chi_{yz} = \frac{1}{4}\left(\frac{\partial^2 v}{\partial y \partial x} - \frac{\partial^2 u}{\partial y^2}\right). \tag{2}$$

We take the defining relations for the panel material in the form:

$$\sigma_{xx} = \frac{E}{1-v^2}\left[e_{xx} + v e_{yy}\right], x \rightleftarrows y, \sigma_{xy} = \frac{E}{(1+v)}e_{xy}, \tag{3}$$

where σ_{ij} are the components of the stress tensor, m_{ij} are components of the moment tensor of higher order, E is Young's modulus, ν is Poisson's ratio, γ is additional independent length parameter.

The equations of the motion of an element of a smooth panel, equivalent to a meshed panel, the boundary and initial conditions are obtained from the Ostrogradsky – Hamilton's energy principle . subject of the study is the meshed panel under the influence of normal distributed load. The panel consists of n sets, densely spaced ribs of the same material. According to the continuum G. I. Pshenichnov's model the regular rib system can be replaced with a continuous layer. The stresses arising in the equivalent smooth panel connected with the stresses in the ribs which make up the angles φ_j with the abscissa axis will have the form:

$$\sigma_{xx} = \sum_{j=1}^{n} \frac{\sigma_x^j \delta_j \mathrm{Cos}^2 \varphi_j}{a_j}, \quad \sigma_{yy} = \sum_{j=1}^{n} \frac{\sigma_x^j \delta_j \mathrm{Sin}^2 \varphi_j}{a_j}, \quad \sigma_{xy} = \sum_{j=1}^{n} \frac{\sigma_x^j \delta_j \mathrm{Cos}\varphi_j \mathrm{Sin}\varphi_j}{a_j},.$$

$$m_{xx} = \sum_{j=1}^{n} \frac{m_x^j \delta_j \mathrm{Cos}^2 \varphi_j}{a_j}, \quad m_{yy} = \sum_{j=1}^{n} \frac{m_x^j \delta_j \mathrm{Sin}^2 \varphi_j}{a_j}, \quad m_{xy} = \sum_{j=1}^{n} \frac{m_x^j \delta_j \mathrm{Cos}\varphi_j \mathrm{Sin}\varphi_j}{a_j}, \tag{4}$$

$$m_{xz} = \sum_{j=1}^{n} \frac{m_{zx}^j \delta_j \mathrm{Cos}\varphi_j}{a_j}, \quad m_{yz} = \sum_{j=1}^{n} \frac{m_{zx}^j \delta_j \mathrm{Sin}\varphi_j}{a_j}$$

Where a_j is distance between edges of j-th sets, δ_j is the thickness of the ribs, voltage index j are rods. Stresses with index j refer to ribs. The physical relations for the meshed plate are determined based on the Lagrange multiplier method (5).

$$\sigma_x^j = \sigma_{xx} \mathrm{Cos}^2 \varphi_j + \sigma_{yy} \mathrm{Sin}^2 \varphi_j + \sigma_{xy} \mathrm{Cos}\varphi_j \mathrm{Sin}\varphi_j; \quad \tau^j = \sigma_{xz} \mathrm{Cos}\varphi_j + \sigma_{yz} \mathrm{Sin}\varphi_j;$$

$$m_x^j = m_{xx} \mathrm{Cos}^2 \varphi_j + m_{yy} \mathrm{Sin}^2 \varphi_j + m_{xy} \mathrm{Cos}\varphi_j \mathrm{Sin}\varphi_j; \tag{5}$$
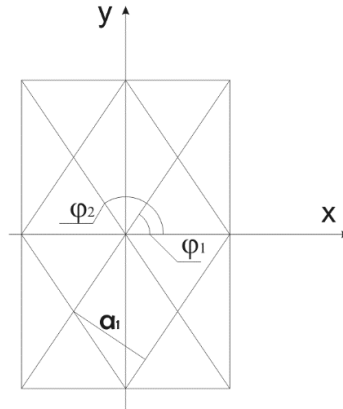

Fig.1. Panel mesh geometry.

The obtained physical relations (5) and expressions which relate the stresses arising in the equivalent smooth panel with the stresses in the ribs (4) will allow us to write the relations for the forces and moments of the smooth panel of the equivalent meshed panel. Substituting the got relations for the forces and moments into the equations of the motion of the smooth panel, we obtain the equations of the motion of the meshed micropolar panel. Later, we will consider the panel with two sets of ribs: $\varphi_1 = 45^o, \varphi_2 = 135^o$, $\delta_1 = \delta_2 = \delta$, $a_1 = a_2 = a$ (Fig.1).

$$2(v-1)\frac{\partial^2 u}{\partial y^2} - 2(3+v)\frac{\partial^2 v}{\partial x \partial y} - 4(v+1)\frac{b^2}{c^2}\frac{\partial^2 u}{\partial x^2} + 4k_y(v+1)\frac{\partial w}{\partial x} + 2(v-1)\frac{\partial^2 w}{\partial y^2}\frac{\partial w}{\partial x} -$$

$$-2(3+v)\frac{\partial w}{\partial y}\frac{\partial^2 w}{\partial x \partial y} - 4(1+v)\frac{b^2}{c^2}\frac{\partial w}{\partial x}\frac{\partial^2 w}{\partial x^2} + \gamma^2(v-1)\left(-\frac{h^2}{b^2}\frac{\partial^4 u}{\partial y^4} + \frac{h^2}{b^2}\frac{\partial^4 v}{\partial x \partial y^3} -\right.$$

$$\left.-\frac{h^2}{c^2}\frac{\partial^4 u}{\partial x^2 \partial y^2} + \frac{h^2}{c^2}\frac{\partial^4 v}{\partial x^3 \partial y}\right) = \frac{8a(v^2-1)}{\delta}\left(\frac{\partial^2 u}{\partial t^2} + \varepsilon\frac{\partial u}{\partial t}\right)$$

$$-4(1+v)\frac{\partial^2 v}{\partial y^2} - 2(3+v)\frac{b^2}{c^2}\frac{\partial^2 u}{\partial x \partial y} + 2(v-1)\frac{b^2}{c^2}\frac{\partial^2 v}{\partial x^2} + 4k_y(1+v)\frac{\partial w}{\partial y} - 4(1+v)\frac{\partial w}{\partial y}\frac{\partial^2 w}{\partial y^2} -$$

$$-2(3+v)\frac{b^2}{c^2}\frac{\partial w}{\partial x}\frac{\partial^2 w}{\partial y \partial x} + 2(v-1)\frac{b^2}{c^2}\frac{\partial w}{\partial y}\frac{\partial^2 w}{\partial x^2} + \gamma^2(v-1)\left(\frac{h^2}{c^2}\frac{\partial^4 u}{\partial x \partial y^3} - \frac{h^2}{c^2}\frac{\partial^4 v}{\partial x^2 \partial y^2} +\right.$$

$$\left.+\frac{h^2 b^2}{c^4}\frac{\partial^4 u}{\partial x^3 \partial y} - \frac{h^2 b^2}{c^4}\frac{\partial^4 v}{\partial x^4}\right) = \frac{8a(v^2-1)}{\delta}\left(\frac{\partial^2 v}{\partial t^2} + \varepsilon\frac{\partial v}{\partial t}\right)$$

$$\left([1+v] + 6\gamma^2[1-v]\right)\frac{c^2}{b^2}\frac{\partial^4 w}{\partial y^4} + 4\left(1+3\gamma^2[v-1]\right)\frac{\partial^4 w}{\partial x^2 \partial y^2} + \left([1+v] + 6\gamma^2[1-v]\right)\frac{b^2}{c^2}\frac{\partial^4 w}{\partial x^4} +$$

$$+12k_y^2(1+v)\frac{c^2}{b^2}w - 12k_y(1+v)\frac{c^2}{b^2}\frac{\partial v}{\partial y} - 12k_y(1+v)\frac{\partial u}{\partial x} + 6k_y(1+v)\frac{c^2}{b^2}\left(\frac{\partial w}{\partial y}\right)^2 -$$

$$-12(1+v)\frac{c^2}{b^2}\frac{\partial w}{\partial y}\frac{\partial^2 v}{\partial y^2} + 12k_y(1+v)\frac{c^2}{b^2}w\frac{\partial^2 w}{\partial y^2} - 12(1+v)\frac{c^2}{b^2}\frac{\partial v}{\partial y}\frac{\partial^2 w}{\partial y^2} - 12(v+1)\frac{\partial^2 w}{\partial y^2}\frac{\partial u}{\partial x} -$$

$$-18(1+v)\frac{c^2}{b^2}\left(\frac{\partial w}{\partial y}\right)^2\frac{\partial^2 w}{\partial y^2} + 6(v-1)\frac{\partial^2 u}{\partial y^2}\frac{\partial w}{\partial x} + 6k_y(v+1)\left(\frac{\partial w}{\partial x}\right)^2 - 12\frac{\partial^2 w}{\partial y^2}\left(\frac{\partial w}{\partial x}\right)^2 -$$

$$-6(3+v)\frac{\partial w}{\partial y}\frac{\partial^2 u}{\partial x \partial y} - 6(3+v)\frac{\partial w}{\partial x}\frac{\partial^2 v}{\partial x \partial y} + 12(v-1)\frac{\partial u}{\partial y}\frac{\partial^2 w}{\partial x \partial y} + 12(v-1)\frac{\partial v}{\partial x}\frac{\partial^2 w}{\partial x \partial y} -$$

$$-48\frac{\partial w}{\partial y}\frac{\partial w}{\partial x}\frac{\partial^2 w}{\partial x \partial y} - 12(1+v)\frac{b^2}{c^2}\frac{\partial w}{\partial x}\frac{\partial^2 u}{\partial x^2} + 6(v-1)\frac{\partial w}{\partial y}\frac{\partial^2 v}{\partial x^2} + 12k_y(v+1)w\frac{\partial^2 w}{\partial x^2} -$$

$$-12(v+1)\frac{\partial v}{\partial y}\frac{\partial^2 w}{\partial x^2} - 12\left(\frac{\partial w}{\partial y}\right)^2\frac{\partial^2 w}{\partial x^2} - 12(1+v)\frac{b^2}{c^2}\frac{\partial u}{\partial x}\frac{\partial^2 w}{\partial x^2} - 18(1+v)\frac{b^2}{c^2}\left(\frac{\partial w}{\partial x}\right)^2\frac{\partial^2 w}{\partial x^2} =$$

$$= \frac{24a(v^2-1)}{\delta}\left(\frac{c^2}{h^2}\frac{\partial^2 w}{\partial t^2} - \varepsilon\frac{c^2}{h^2}\frac{\partial w}{\partial t} - 2q\right).$$

(6)

Initial and boundary conditions should be added to the equations.

In the experiments were taken the zero initial conditions and the fixed boundary conditions:

$$u = v = w = 0, \frac{\partial u}{\partial x} = 0, \frac{\partial u}{\partial y} = 0, \frac{\partial v}{\partial x} = 0, \frac{\partial v}{\partial y} = 0, \frac{\partial w}{\partial x} = 0, \frac{\partial w}{\partial y} = 0 \quad npu \quad x = \pm 1, y = \pm 1. \tag{7}$$

Static problems in the theory of plates and shells have traditionally been solved using various approximate methods. They allow to modify the system of partial differential equations to the system of nonlinear algebraic equations, which is further linearized. In this article, the solution of static problems will be presented using the establishment method, which was for shells by I.V. Feodosiev first applied. In the method of establishing setting, the solving of the system of partial differential equations reduces to solving the Cauchy problem for the system of ordinary differential equations, which is initially linear in time. This approach has some advantages. The establishment method has high accuracy, as it can be related to iterative methods. Here, each time step is new approximation to the exact solution of the problem. In addition, the establishment method isn't very sensitive to the initial choice of the approximation. Solving the Cauchy problem for $\varepsilon = \varepsilon_{\kappa p}$, for the number of values of the normal time constant w_i. parameter of the load q_i, we obtain the sequence of deflections Based on these data, the relationship $w(q)$ is constructed and the stress-strain state of the system is studied. It should be noted that it is necessary to pay serious attention to the choice $\varepsilon_{\kappa p}$.

In some cases, if energy dissipation is not taken into account, the critical dynamic value of the load can be approximately half the static critical value of the load. In this article, for to solve the static problem, the system of partial differential equations was reduced in spatial coordinates by the finite difference method with a second-order approximation to the Cauchy problem. The Cauchy problem was solved by Newmark's method. It was experimentally chosen $\varepsilon_{\kappa p} = 10$. This value gives the smaller number of iterations solving the problem by the establishment method.

When solving problems in mechanics numerically, the results are presented in the form of numerical tables. The analysis of the results in this form causes great difficulties. For the qualitative assessment of the information contained in the tables, its high-quality graphic visualization is necessary. In this work, the software used Autodesk 3ds Max. Compared to the many existing programs developed for visualization of numerical solutions, Autodesk 3ds Max has a large set of utilities that allow you not only to get good image resolution, but also to get creative with the visualization itself. Apply various effects to the image: multi-colored lighting from different angles, add a specular reflection to the image.

3 Numerical experiment

Consider a mesh cylindrical panel under the action of a transverse uniformly distributed static load. Fig. 2-3 shows of the dependence "static load-deflection".

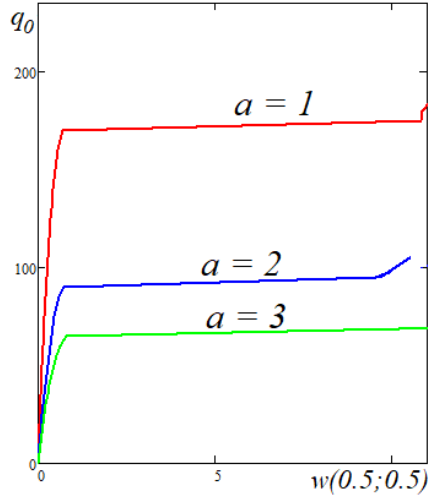The studies were carried out depending on the increase in the distance between the

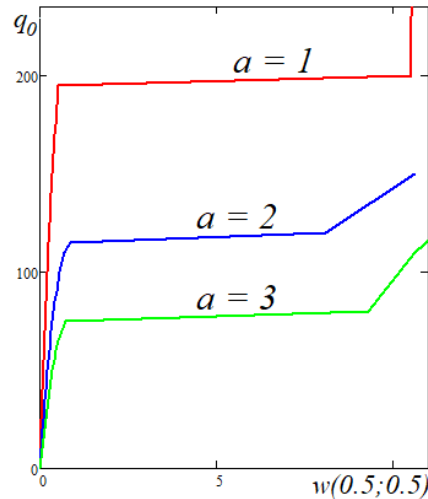**Fig. 2.** "Load-deflection" relationship ($\gamma = 0$).

Fig. 3. "Load-deflection" relationship» ($\gamma = 0.5$).

edges $a = 1, 2, 3$ for a mesh panel with curvature parameters $k_y = 48$. As the distance
between the panel edges increases, the structure becomes softer, i.e. the bearing panel
Only two levels of headings should be numbered. Lower level headings remain unnumbered; they are formatted as run-in headings.

becomes softer, i.e. the bearing panel capacity decreasing. The increase in the distance between the panel edges did not affect the panel bending form, as well as the
diagrams of moments and forces under subcritical and supercritical loads. An increase
in the size-dependent parameter increases the bearing capacity of the panel.

Process visualization of the static stability loss was carried out using the Autodesk
3ds Max program. The table 1-2 shows the diagrams of deflection, average moment
$\left(M_{avg} = \dfrac{M_x + M_y}{2} \right)$ and average forces $\left(N_{avg} = \dfrac{N_x + N_y}{2} \right)$ of the panel at a load of
$q_0 = 40$ (subcritical load) and after "clap" at $q_0 = 120$ (supercritical load), at a=3 and
a size-dependent parameter $\gamma = 0; 0.5$.

At $q_0 = 40$, the deflection plot has a dome-shaped shape, after "clap" at $q_0 = 120$,
the shape is also dome-shaped, but the apex is sharper.

The visualization of the moment shows that before the "clap", the moment values in
the center of the shell are positive, while the moment values are negative at the edges
of the shell. The moment diagram changes shape after the "clap". The visualization of
the results the results the "clap". The visualization of the results shows that after the
"clap", the moment has a maximum value in the center of the shell.

Static buckling leads to a change in the shape of the force diagram. After the "clap" forces in the quarters change sign. The graphs show that with the value of the size-dependent parameter, changes in the distribution of forces in the shell are more pronounced.

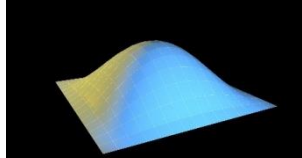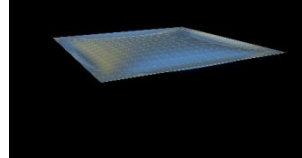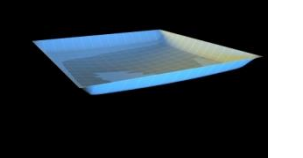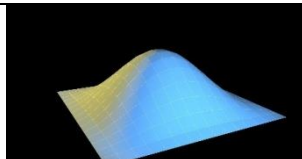**Table 1.** Diagrams of deflections, moments and forces for the shell $\gamma = 0$.
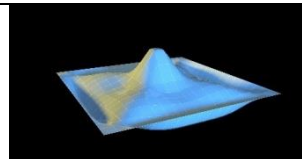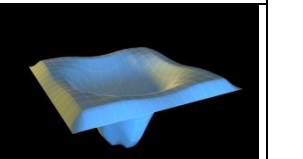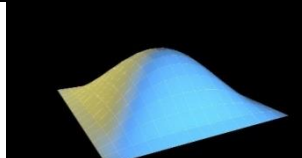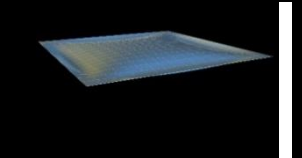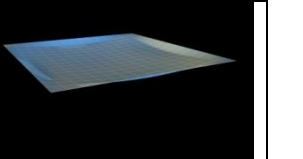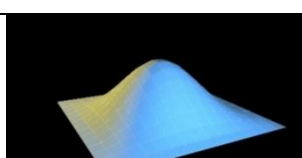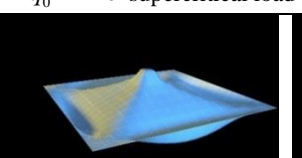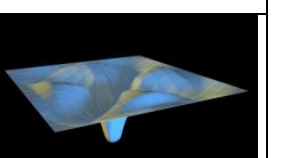
Panel deflection	Panel moment	Efforts in panel
$q_0 = 40$ subcritical load		
$q_0 = 120$ supercritical load		

Table 2. Diagrams of deflections, moments and forces for the shell $\gamma = 0.5$

Panel deflection	Panel moment	Efforts in panel
$q_0 = 40$ subcritical load		
$q_0 = 120$ supercritical load		

4   Conclusion

The article presents a visualization of the process of loss of static stability of a cylindrical panel with a micropolar mesh. Static buckling is accompanied by a change in the diagrams of moments and forces at the subcritical and supercritical points. Changes

in the force diagrams are more noticeable when moment stresses are taken into account. Visualization of the results using 3B made it possible to establish that an increase in the distance between the edges of the mesh panel and an increase in the parameter depending on the size does not change the bending shape of the panel, as well as the diagrams of moments and forces at subcritical and supercritical loads.

References

1. Safarpour, H., Mohammadi, K., Ghadiri, M.: Temperature-dependent vibration analysis of a FG viscoelastic cylindrical microshell under various thermal distribution via modified length scale parameter: a numerical solution. Journal of the Mechanical Behavior of Materials 26, 9–24 (2017)
2. Sahmani, S., Ansari, R., Gholami, R., Darvizeh, A.: Dynamic stability analysis of functionally graded higher-order shear deformable microshells based on the modified couple stress elasticity theory Composites Part B. Engineering 51 44–53 (2013)
3. Varygina, M.: Numerical modeling of micropolar cylindrical shells on supercomputers with GPUs AIP Conference Proceedings 1895, 080005 (2017)
4. Zhou, X., Wang, L.: Vibration and stability of micro-scale cylindrical shells conveying fluid based on modified couple stress theory. Micro & Nano Letters 7(7), 679– 684 (2012)
5. Krylova, E. Yu, Papkova, I. V, Sinichkina, A. O., Yakovleva, T. B., Krysko-yang, V. A.: Mathematical model of flexible dimension-dependent mesh plates. IOP Conf. Series: Journal of Physics: Conf. Series 1210 (2019) 012073 doi:10.1088/1742-6596/1210/1/012073
6. Krysko, V.A., Papkova, I.V., Krysko, A.V., Krylova, E.Yu.: Visualization of transition's scenarios from harmonic to chaotic flexible nonlinear-elastic nano beam's oscillations. CEUR Workshop Proceedings 62-65 (2019)
7. Azarov, A.V.: Continuum model of composite mesh shells formed by a system of spiral edges. Composites and nanostructures. V. 7, 3 (27), 151-161. (2015)
8. Belikov, G. I.: General case of bending of a rectangular mesh plate taking into account the tensile forces acting in the middle surface. Bulletin of the Volgograd state University of architecture and civil engineering. Series: Construction and architecture. 37 (56), 121-128. (2014)
9. Azikov, N. With. Pavlov E. A.: stability Study of a mesh composite plate. Aviation industry. 3, 46-50. (2016)
10. Burnysheva, T. V., Steinbrecher, O. A., Ulyanov, A. D.: Aspects of specifying boundary conditions in the simulation mesh anisogamy designs. Bulletin of the South Ural state University. Series: Mathematical modeling and programming. 11(1), 137-144. (2018)
11. Trushin, S.I., Zhuravleva, T.A., Sysoeva, E.V.: Dynamic loss of stability of nonlinear deformable grid plates made of composite material with different lattice configurations. Scientific review. 4, 44-51 (2016)
12. Zinin, A.V., Azik, N.: The model of destruction process of composite structures anisakidae problems. Mechanical engineering and reliability of machines. 5, 49-56. (2018)
13. Mindlinand, R. D., Tiersten, H. F.: Effects of couple-stres sesin linear elasticity. Arch. Ration.Mech. Anal.11, 415–448 (1962).
14. Nikabadze, M.U.: Some versions of equations of micropolar shell theories // Applied Mathematics and Mathematical Physics. 1(1), 101-118. (2015)
15. Sargsyan, S.H., Zhamakochyan, K.A.: Applied theory of micropolar elastic thin plates with constrained rotation and the finite element method. Materials Physics and Mechanics. 35(1), 145-154 (2018)

16. Toupin, R. A.: Elastic materials with couple-stresses. Arch. Ration. Mech. Anal. 11, 385–414 (1962)
17. Eringen, A. C.: Nonlocal polarelastic continua. Int. J. Eng. Sci. 10, 1–16 (1972)
18. Kurt, I., Kaya, M.O.: Flapwise Bending Vibration Analysis of a Double Tapered Rotating Nonlocal Euler-BernoullI Beam by the Differential Transform Method. Journal of Applied Mechanics and Technical Physics. V. 60, 5 (357), 206-216 (2019)
19. Mikhasev, G.I., Sheiko, A.N.: Simulation of free vibrations of multi-walled carbon nanotube based on non-local theory of thin elastic orthotropic shells. Mechanics of machines, mechanisms and materials. 4 (25). 60-64. (2013)
20. Aifantis, E. C.: Strain gradient interpretation of size effects. Int. J. Fract. 95, 299–314 (1999)
21. Gurtin, M. E., Weissmuller, J., Larche, F.: Thegeneral theory of curved deformable einterfaces in solid sat equilibrium. Philos. Mag. A 78, 1093–1109 (1998)
22. Wu, Q.L., Zhang, W., Dowell, E.H.: Detecting multi-pulse chaotic dynamics of high-dimensional non-autonomous nonlinear system for circular mesh antenna. International Journal of Non-Linear Mechanics 102, 25–40 (2018)
23. dell'Isola, F., Steigman, D. A: Two-dimensional Gradient-Elasticity Theory for Woven Fabrics. J. Elast. V. 118, 1 113–125 (2015)
24. Eremeev, V. A: On a nonlinear model of the mesh shell. Izvestiya of the Russian Academy of Sciences. Solid mechanics. 4. 127-133 (2018)
25. Krylova, E.Yu., Papkova, I.V., Saltykova, O.A., Sinichkina, A.O., Krysko, V.A.: Mathematical model of oscillations of dimensionally dependent cylindrical shells of a mesh structure taking into account the Kirchhoff-Love hypotheses Non-linear world 16(4), 17-28 (2018)
26. Krylova, E.Yu., Papkova, I.V., Saltykova, O.A., Krysko, V.A.: visualization of scenarios for the transition of oscillations from harmonic to chaotic for a micropolar Kirchhoff-Love cylindrical meshed panel. CEUR Workshop Proceedings 66-70 (2019)